Eur Biophys J (2009) 38:891–901
DOI 10.1007/s00249-009-0463-8

ORIGINAL PAPER

Cell–surface interactions involving immobilized magnetite nanoparticles on flat magnetic substrates

Juliane Loichen · Uwe Hartmann

Received: 2 November 2008 / Revised: 19 March 2009 / Accepted: 28 April 2009 / Published online: 2 June 2009

Abstract A new method to affect cells by cell–surface interaction is introduced. Biocompatible magnetic nanobeads are deposited onto a biocompatible magnetic thin layer. The particles are composed of small magnetite crystals embedded in a matrix which can be functionalized by different molecules, proteins or growth factors. The magnetic interaction between surface and beads prevents endocytosis if the setup is utilized for cell culturing. The force acting between particles and magnetic layer is calculated by a magnetostatic approach. Biocompatibility is ensured by using garnet layers which turned out to be nontoxic and stable under culturing conditions. The garnet thin films exhibit spatially and temporally variable magnetic domain configurations in changing external magnetic fields and depending on their thermal pretreatment. Several patterns and bead deposition methods as well as the cell–surface interactions were analyzed. In some cases the cells show directed growth. Theoretical considerations explaining particular cell behavior on this magnetic material involve calculations of cell growth on elastic substrates and bending of cell membranes.

Keywords Cell–surface interaction · Magnetic film · Nanoparticles · Magnetic particles · Directed growth · Cell membrane

Introduction

For several years it has been known that cell growth is influenced by structures at the micrometer to nanometer scale (Curtis and Wilkinson 1997; Curtis and Riehle 2001). In tissue engineering the influence of cells through cell–surface interactions is considered as a promising biotechnological route. Cell behavior as a response to substrate properties and the systematic employment of surface structuring to adsorb cells in a controlled manner is also a matter of current biomedical research, especially in implant technology (Sato and Webster 2004) or stem-cell-related approaches. Substrate modifications can usually involve chemical, mechanical or topographical features (Wong et al. 2004). The most accurate geometrical control of cell growth can be achieved by using chemical structuring, where defined areas allow for adhesion while others prevent it (Cavalcanti-Adam et al. 2007; Théry et al. 2006). Topographical structures can cause cell alignment, influences on growth and adhesion, or even apoptotic behavior. These are accompanied by modifications of inter- and intracellular signalling (Dalby et al. 2003, 2004). Cell alignment along grooves and ridges in general is a well-known phenomenon (Curtis and Wilkinson 1997; Yu et al. 2005; Teixeira et al. 2003), which is observed if the dimension of the characteristic topographic features is comparable to the cell size or smaller. Mechanical properties of biocompatible substrates influence the cell behavior as well (Wong et al. 2004). Cells are sensitive to different elasticities or a directed tension of the substrates. It could be shown that cells align along the axis of strain or move to areas of highest stiffness (Lo et al. 2000; Schwarz and Safran 2002; Takakuda and Miyairi 1996). To investigate the cellular response to different elasticities, materials with gradients in stiffness and substrate deformations as a result of externally applied forces were used (Lo et al. 2000; Takakuda and Miyairi 1996).

A large number of structuring methods to induce chemical and/or topographical variations have already been

J. Loichen (✉) · U. Hartmann
Institute of Experimental Physics, Saarland University,
66123 Saarbrücken, Germany
e-mail: j.loichen@gmx.net

developed. Lithographic techniques are time consuming but accurate. Electron-beam lithography, laser interference (Yu et al. 2005), and photolithography (Teixeira et al. 2003; Barbucci et al. 2002) have been employed. These allow topographical patterning of hard materials without further chemical procedures. Another successful method in cell culturing is the employment of self-assembled structures (Mrksich and Whitesides 1996; Arnold et al. 2004). A frequently used approach for biochemical structuring is soft lithography (Xia and Whitesides 1998). Proteins are transferred to substrates in certain patterns using soft stamps, either for creating binding sites for proteins or for transferring proteins directly into ordered structures for controlled cell adhesion.

Recently a new method for cell cultivation was introduced which allows for in vitro and in situ topographical changes (Issle and Hartmann 2007, 2008; Issle and Hartmann patent pending). Magnetite nanobeads, which can be chemically functionalized, are immobilized on biocompatible magnetic thin films, i.e., on garnet layers. The particular, variable domain configurations of the garnets allow for an externally defined physical immobilization of the particles. The substrates have a strong perpendicular anisotropy and can be used in cell culture without any toxic effects. As a result living cells can be influenced by spatially and temporally varying topographical and biocompatible "landscapes." The magnetic interaction between the substrate and the nanoparticles is strong enough to prevent endocytosis.

Chemical structuring depends on the particular kind of functionalization of the nanobeads. However, below, the main focus is the direct influence of the substrate and the particles on the cells. The utilized particle patterns constitute a purely topographical and mechanical "landscape." The influence on cell growth is studied by comparing experimentally obtained data with theoretical approaches based on cell mechanical models.

The proposed approach establishes a completely new combination of materials to be used in cell culture experiments. The following study confirms that the involved materials are nontoxic and that the internalization of functionalized and nonfunctionalized nanoparticles by cells is prevented. It is also shown that the employed cells are not affected by the strong magnetic fields provided by the utilized magnetic substrates. They do, however, show directed growth as a result of externally defined patterns of magnetic particles. In its versatility the proposed setup can be used as an experimental platform to perform a variety of experiments on cell–surface interactions, shedding further light on the question of to what degree control of cell functions is possible via the extracellular matrix. The experiments can involve solely mechanical properties being defined by the patterns of magnetic composite particles on the magnetic substrate. They can, however, also involve particles with biochemical functionalization. The following discussion mainly focuses on the influence of topographical and mechanical surface properties on cell growth.

Experimental approach

Substrate

The yttrium iron garnet of composition $Y_3Fe_5O_{12}$ is ferrimagnetic with usually cubic anisotropy. In our approach a strong perpendicular anisotropy is preferred. This can be obtained by substituting some of the Y by Bi ions. Concretely, layers of the composition $Y_{2.5}Bi_{0.5}Fe_{5-\delta}Ga_{\delta}O_{12}$ ($\delta = 0.5$–1), which were grown on a paramagnetic (111) gadolinium gallium garnet by liquid-phase epitaxy, were used. The film thickness is 4–6 μm. The saturation magnetization M_S, as determined by vibrating sample magnetometry, is of the order of 1.5×10^4 A/m. Without any externally applied magnetic fields, particular metastable domain configurations are observed. Each domain is magnetized out of plane and antiparallel to adjacent domains. Figure 1 shows these magnetic configurations as observed by Faraday microscopy. Figure 1a represents the garnet layer in its most stable configuration, i.e., exhibiting the maze domain pattern. By a temperature pretreatment (heating above the Curie temperature of approximately 425 K and cooling afterwards in either zero or inhomogeneous fields at different angles with respect to the film surface) one obtains stripe domains (Fig. 1b), bubbles (Fig. 1c) or the mixed state (Fig. 1d). All states appear to be stable in the absence of external fields. The transformation of one state into another can be performed solely by applying suitable magnetic fields (Hubert et al. 1974). The details are described in Issle and Hartmann (2008). A theoretical treatment is given in Hubert et al. (1974) and Hubert and Schäfer (1998). One particular advantage of the approach is the possibility of in vitro and in situ modification of the domain configuration by means of external magnetic fields. For this purpose a climate chamber with a coil system (to produce controllable homogenous magnetic fields) was integrated into an optical microscope. Cell cultivation can be carried out under standard conditions over several days, whereby the magnetic conditions can be varied. The garnet layer is transparent for visible light, which is an advantage for biological investigations involving a transmission light microscope.

Nanoparticles

Biocompatible magnetic composite nanoparticles were deposited onto the substrate. The fluidMAG-ara particles (chemicell, Berlin, Germany) consist of small magnetite

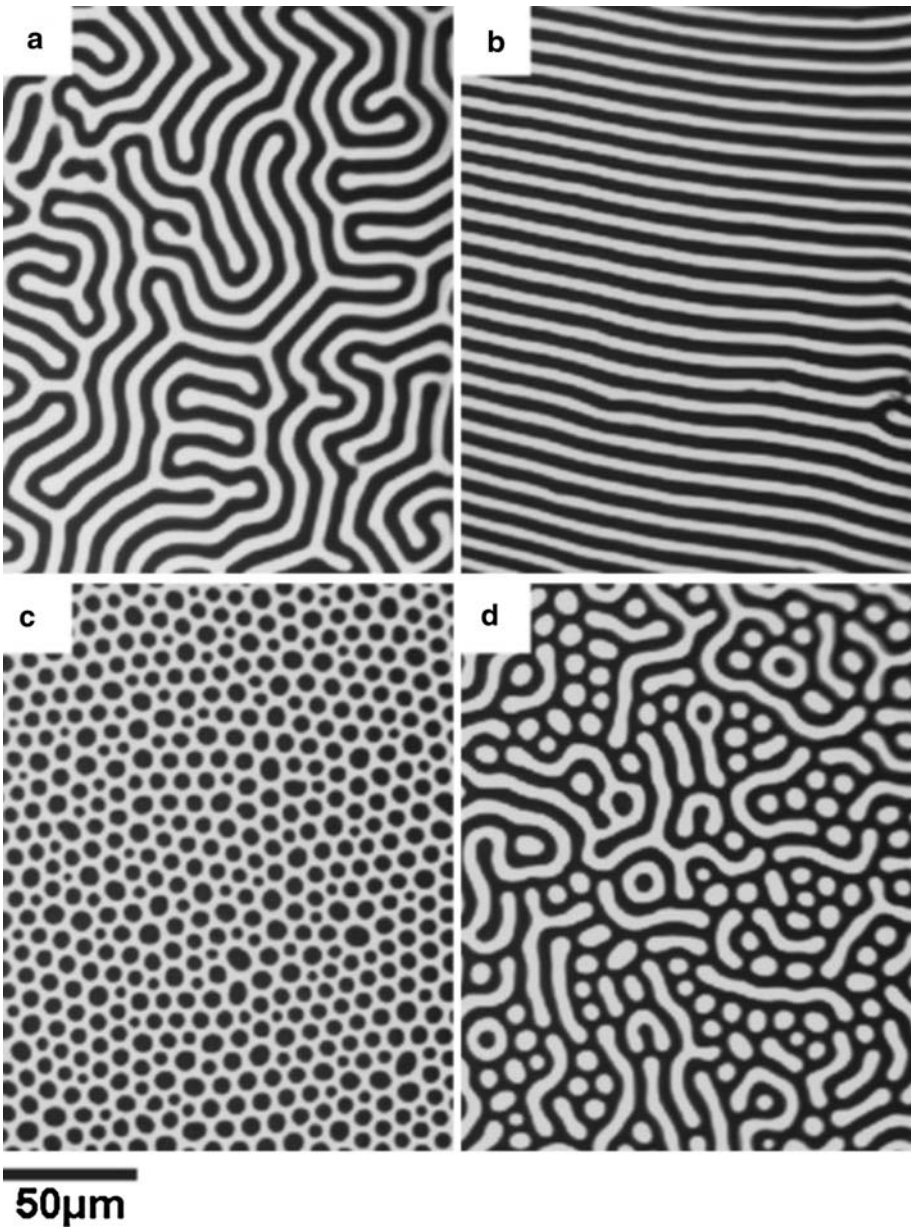

Fig. 1 Metastable domain configuration of a garnet layer. **a** Maze domain pattern or labyrinthine structure, **b** stripes, **c** bubbles, and **d** mixed pattern. The antiparallel domains are imaged by Faraday microscopy

(Fe_3O_4) crystals with a diameter of approximately 12 nm, embedded in a biocompatible polysaccharide matrix. This enables stability and prevents biodegradation for several days up to weeks. Magnetite is known to be completely biocompatible. It does not show any toxicity (no L_{50} index) (Berry and Curtis 2003). The shell allows for covalent binding of growth factors or other proteins of interest so that the particles can be functionalized. The average diameter of the particles is approximately 150–200 nm, whereas the volume fraction of magnetite within a composite particle is 80%. A composite particle is not a perfect sphere; it is randomly shaped due to the fact that the magnetite particles are held together only by a thin shell. The maximum size specified by the manufacturer is 250 nm. This fact could be proven by atomic force microscopy (AFM) measurements on immobilized particles. The height of the particles in such measurements is around 200 nm but not higher than 250 nm. The size distribution of the single crystals was determined by transmission electron microscopy (TEM). The radius is 6 ± 0.9 nm based on the investigation of 300 crystallites. A TEM image of a composite particle is shown in Fig. 2. The single crystals are clearly visible, whereas the shell does not provide any contrast. The crystallites are small enough to consist of single magnetic domains and to behave superparamagnetically at room temperature. From superconducting quantum interference device (SQUID) measurements we found that the composite particles are superparamagnetic with a susceptibility of about $\chi = 12$ in magnetic fields up to 5×10^4 A/m at room temperature.

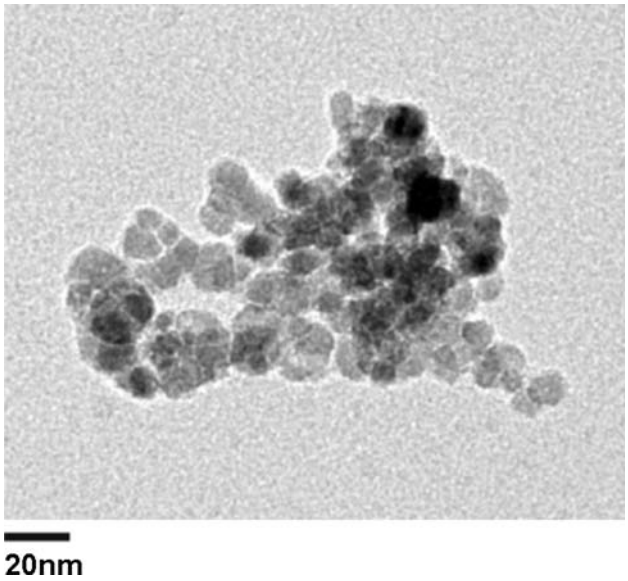

Fig. 2 Transmission electron micrograph of a nanoparticle. Single magnetite crystals in the range of 12 nm in diameter are visible, whereas the polysaccharide shell in which the crystals are embedded does not provide any contrast

Due to their magnetic behavior the particles can be tightly adsorbed to the magnetic garnet layers. If the particles are kept in water or suspended in inorganic liquids they can be transferred by adding a droplet onto the magnetic layer which is likewise kept under liquid environment. Through the magnetic forces the particles bind to the garnet layer. The excess particles which are not strongly bound are removed by performing several washing steps. Thus, the liquid environment of the garnet layer is exchanged several times. Thereby, a regular particle pattern according to the specific domain structure can be obtained.

Advanced deposition methods

Even more flexibility in the selection of areas for particle deposition is obtained by combining domain patterning with soft lithography (Issle and Hartmann 2008). For this purpose poly(dimethylsiloxane) (PDMS) stamps with geometrically well-defined structures in the micron range were employed. The cavities of such stamps serve as microfluidic channels if the stamp is in contact with the flat garnet layer before adding the particle suspension to the edges between surface and stamp. Alternatively a droplet of particle suspension is put onto the garnet layer and afterwards the stamp is pressed onto the magnetic layer. The exposed areas of the stamp which are in direct contact with the substrate are used for displacing the particle suspension, whereas the cavities allow for particle adsorption. More details are given by Issle and Hartmann (2008). For the present approach the stamp profiles consist of lines of 20 µm width and 40 µm periodicity or of octagons of 50 µm width and 54 µm center-to-center distance. In Fig. 3 garnet layers with deposited particles are shown. The particles are deposited in the areas which correspond to the cavities of the used stamps. They agglomerate on the domain walls of the specific structure. Figure 3a shows a linear superstructure superimposed onto a mixed domain pattern, whereas Fig. 3b shows an octagon superstructure superimposed onto stripe domains.

Cell culture

Substrate structuring as described can be used in cell culture. For MG63 osteoblasts (ATCC CRL-1427) Dulbecco's modified Eagle's medium (DMEM) high-glucose

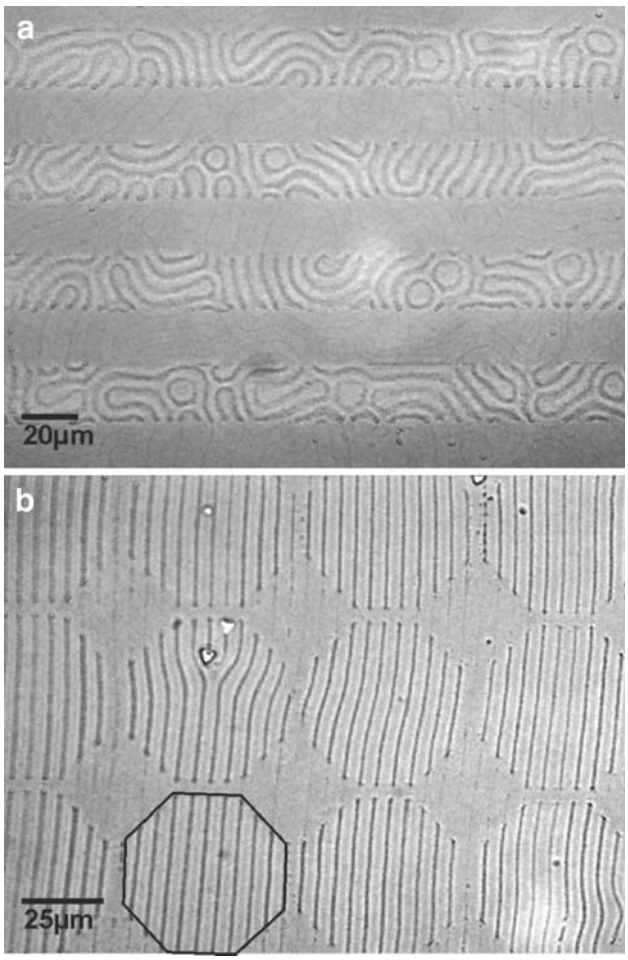

Fig. 3 Magnetite particles are deposited on a garnet layer in geometrically well-defined areas. The *black lines* correspond to agglomerated particles on domain walls. Light microscopic image of **a** a linear particle superstructure of 20 µm width of a mixed domain pattern and **b** an octagon superstructure of stripe domains

medium was used, supplemented with 10% fetal bovine serum (FBS), 1% penicillin/streptomycin, and 100 mg/l sodium pyruvate (all from PAA, Pasching, Austria). The cells were investigated up to 7 days during one experiment and the medium was exchanged every 48 h. Osteoblasts were chosen as a first feasibility study. They are a well-characterized and well-understood cell type which are known to be sensitive to topographical influences. Studies on other cell types which show different adherence properties are not covered herein. A low seeding density was chosen so that after seeding the cells were isolated from each other and single-cell observation was possible. This could be ensured by a density of approximately 2.5×10^3 cells/cm^2.

Results and discussion

Particle immobilization

The simplest case in the calculation of the magnetic interaction between the particles and the garnet layer is the linear stripe domain pattern, shown schematically in Fig. 4. In the experiments, garnet layers of 5 μm thickness and domain width of 5 μm were used. In the stray-field calculations the thickness of the magnetic layer is assumed to be infinite. This is justified because the radius of the particles defines the distance of interest. The latter is 100 nm and is thus well below the layer thickness. The stripes are parallel to the y direction such that the magnetic field and force distributions are within the x–z plane. The magnetization $M(x)$ along the x direction is given by the Fourier series of a square-wave signal with amplitude M_S and by defining $k := \pi/d$:

$$M(x) = \frac{4M_S}{\pi}\left(\sin kx + \frac{\sin 3kx}{3} + \frac{\sin 5kx}{5} + \cdots\right). \quad (1)$$

This leads to the magnetic field components H_x and H_z above the magnetic layer as indicated in Fig. 4:

$$H_z(x,z) = \frac{2M_S}{\pi}\sum_{n=0}^{\infty}\frac{1}{2n+1}\exp[-k_n z]\sin[k_n x], \quad (2)$$

$$H_x(x,z) = \frac{-2M_S}{\pi}\sum_{n=0}^{\infty}\frac{1}{2n+1}\exp[-k_n z]\cos[k_n x], \quad (3)$$

where z is the height above the garnet layer and $k_n := (2n+1)k$. For particle deposition the height is $z = 100$ nm according to the particle radius. The respective field distribution is shown in Fig. 5a. Domain walls are assumed at position $x = 0$ μm, ±5 μm. H_z is largely constant above the domains. H_x is zero in the center of the domains and has a maximum above the domain walls. In order to calculate the force which acts on a particle which is in contact with the magnetic layer, a spherical particle of radius $r = 100$ nm is taken into account. As the magnetization of the superparamagnetic particles changes linearly in external fields, the magnetic moment $\mathbf{m}$ of one composite particle of volume V in an external magnetic field $\mathbf{H}$ is given by $\mathbf{m} = V\chi\mathbf{H}$. Thus, the force $\mathbf{F} = -\nabla\phi$, arising from the potential ϕ of a particle in the magnetic field of the garnet layer, is $\mathbf{F} = \mu_0\nabla(\mathbf{m}\cdot\mathbf{H}) = \mu_0 V\chi\nabla H^2$. The components of this force are

$$F_x = \mu_0 V\chi\frac{8M_S^2}{\pi^2}\left[\begin{array}{l}\displaystyle\sum_{n=0}^{\infty}\left(\frac{1}{2n+1}\exp(-k_n z)\cos(k_n x)\right)\sum_{n=0}^{\infty}\left(-k\exp(-k_n z)\sin(k_n x)\right)\\ \displaystyle+\sum_{n=0}^{\infty}\left(\frac{1}{2n+1}\exp(-k_n z)\sin(k_n x)\right)\sum_{n=0}^{\infty}\left(k\exp(-k_n z)\cos(k_n x)\right)\end{array}\right], \quad (4)$$

$$F_z = \mu_0 V\chi\frac{8M_S^2}{\pi^2}\left[\begin{array}{l}\displaystyle\sum_{n=0}^{\infty}\left(\frac{1}{2n+1}\exp(-k_n z)\cos(k_n x)\right)\sum_{n=0}^{\infty}\left(-k\exp(-k_n z)\cos(k_n x)\right)\\ \displaystyle-\sum_{n=0}^{\infty}\left(\frac{1}{2n+1}\exp(-k_n z)\sin(k_n x)\right)\sum_{n=0}^{\infty}\left(k\exp(-k_n z)\sin(k_n x)\right)\end{array}\right]. \quad (5)$$

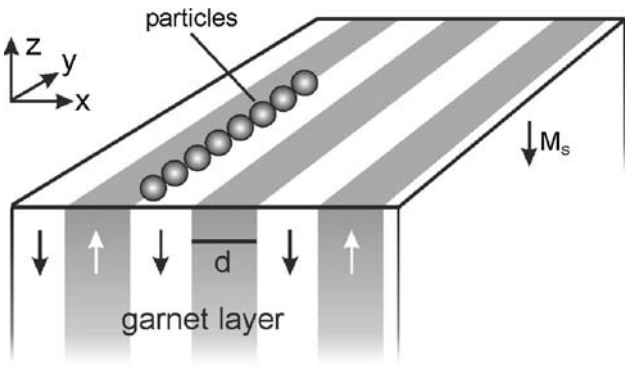

Fig. 4 Schematic drawing of a stripe domain pattern of a garnet layer of infinite thickness, domain width d, and magnetization M_S. Particles agglomerate at domain walls

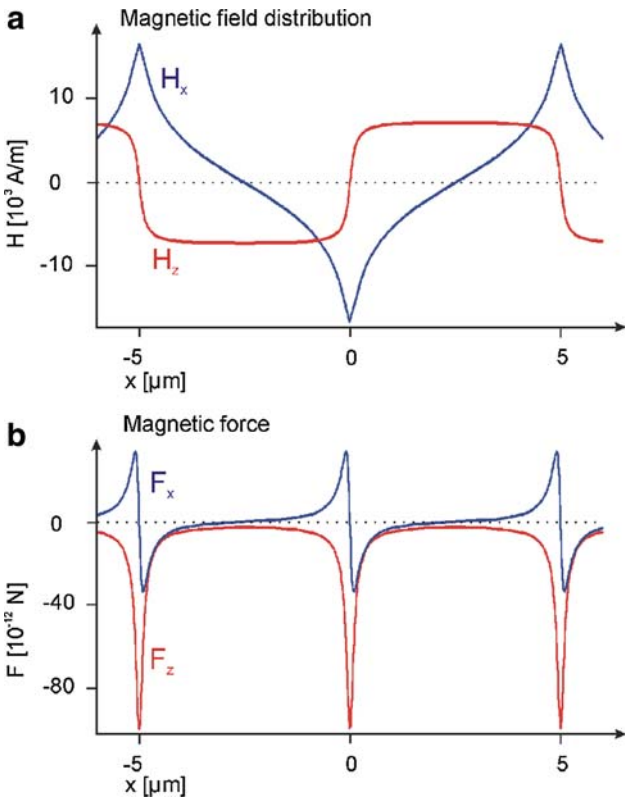

Fig. 5 **a** Calculated lateral (H_X) and vertical (H_Z) magnetic field distribution 100 nm above the garnet film and **b** components of the force acting between particles and magnetic layer

Results of numerical calculations are shown in Fig. 5b. The vertical component is always attractive towards the substrate surface. Above a domain wall it is almost 90 pN. The lateral component vanishes at the center of the domains. A particle is attracted either to the left or to the right towards the next domain wall. The strongest lateral force of approximately 33 pN is reached at a distance of 90 nm from the domain wall. According to the calculations it should be possible for a particle to adhere to the surface of the garnet layer everywhere as it is always attracted by F_x. In cell culture experiments it is not useful to cover the whole surface with particles because a cell can internalize weakly bound beads by endocytosis (Rejman et al. 2004). Before using the substrates in cell culture the excess particles which are not strongly bound to the magnetic surface are removed by several washing steps. This leads to the structures shown in Fig. 3. Atomic force and scanning electron microscopy showed that the width of the particle deposition on top of a domain wall is 800 nm to 1 µm at maximum with a corresponding total magnetic force of 18 pN. Consequently, by the washing steps, the amount of particles is reduced to five particles across a domain wall if an average particle radius of 100 nm is assumed. $F_x(x)$ shows a linear behavior along 50 nm on both sides of a domain wall and can thus be expressed by $F_x(x) = -Dx$. The respective elasticity is $D = 6.7 \times 10^{-4}$ N/m. This is of importance for the following discussion.

Biocompatibility and anisotropic cell growth

The garnet layer and the magnetically immobilized particles turned out to be absolutely biocompatible under cell culture conditions. The monocrystalline substrate is long-term stable in the culture and the toxic components of the compound do not dissolve. In conjunction with the transparency for visible light, the garnets are ideal atomically flat substrates for cell experiments. The particles are used in biomedical research and are used for medical diagnosis and therapies, e.g., in hyperthermia (Lu et al. 2007). Thus they are known to be nontoxic. After magnetic immobilization on the garnet layer, cells cannot internalize the particles. This could be proven by cross sections of cells with a focused ion beam. In Fig. 6, left image, cells are shown which were cultivated for 3 days on a glass substrate with deposited particles. It is clearly visible that the particles are internalized and located in the cell. The contrary situation is shown in Fig. 6, right image. There the cells were cultivated on magnetic garnet layers with immobilized particles. The particles are still bound to the domain walls and the cell membrane is spread over the particles and not around them. Osteoblasts grown on the substrate with deposited nanoparticles are shown in Fig. 7. Over several days in culture the cells grow until confluency. The time to reach cell confluency depends on the seeding density at the beginning of the experiment. For reasons of comparison the same densities were used for growth on garnet layers and glass substrates, respectively. Confluency was in both cases reached at the same time after starting the experiment, usually after 4 days. The domain structure itself, and therewith the particle structure, does not have any visible influence on cell growth. Cells grow uniformly without preferred direction on a layer

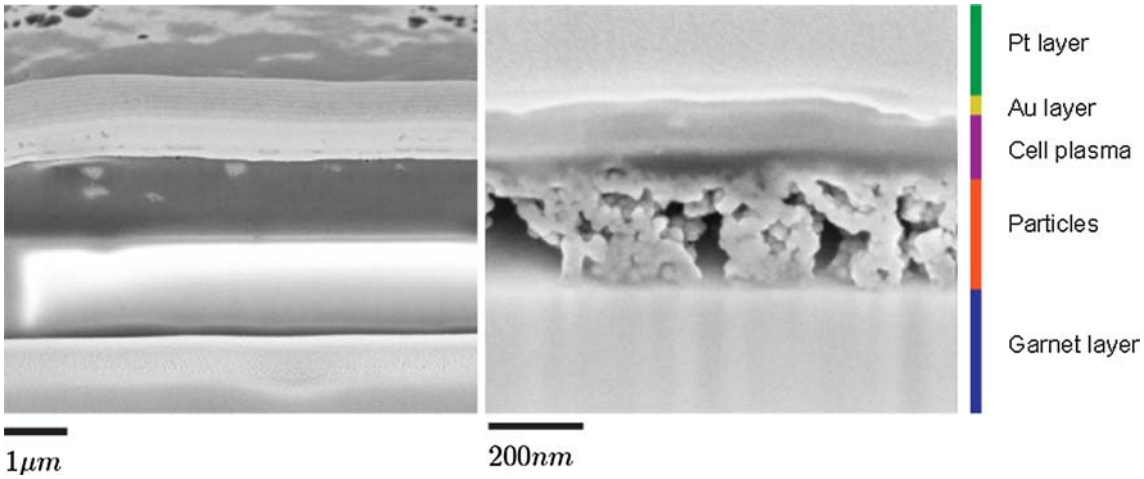

Fig. 6 *Left* FIB cross section of a cell on a glass substrate with internalized particles. *Right* cell on garnet layer with magnetically immobilized particles. The magnetic interaction between the substrate and the particles is strong enough to inhibit endocytosis

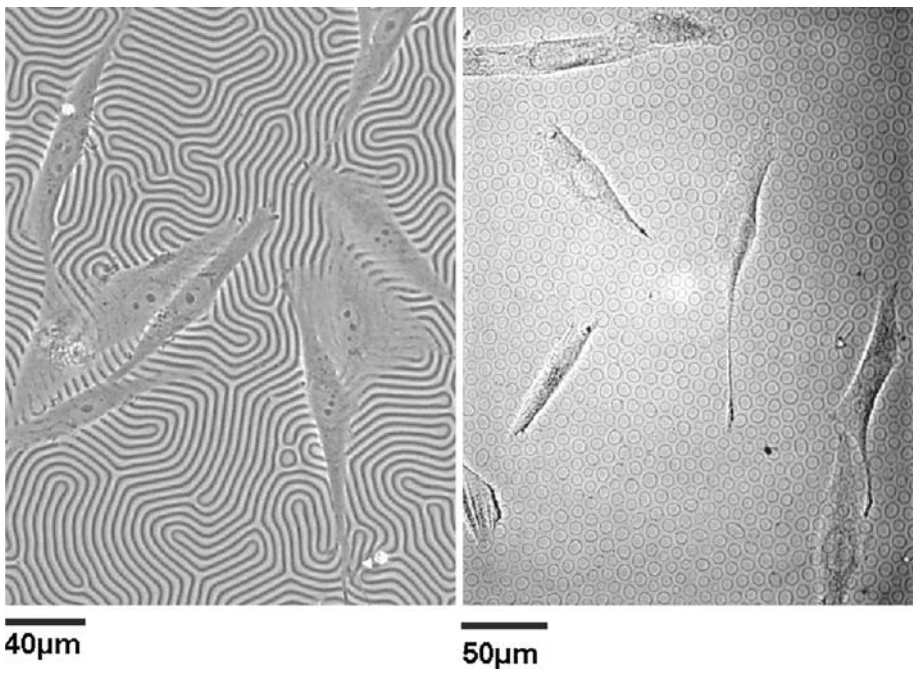

Fig. 7 Osteoblasts on a garnet layer with deposited beads. The cells grow well until confluency within several days and exhibit uniform growth. The *black lines* are deposited beads on the domain walls of a labyrinthine pattern or bubble domain structure, respectively

exhibiting the labyrinthine structure (Fig. 7, left) or the bubble domain structure (Fig. 7, right). The cell shape is flat as expected for adherent cells such as osteoblasts. As they are not spherically shaped the cells can adhere to the particles as well as to the garnet layer.

In order to gain better control in treating cells with different proteins or growth factors via functionalized particles, the aforementioned stamp-based methods can be applied to create areas with and without immobilized particles. The superstructures enable one to distinguish cells in contact with the biochemical agents from those growing on the naked substrate under otherwise identical conditions. This is important in stem cell research, where spontaneous differentiation has to be distinguished from controlled triggered differentiation. For that particular purpose various methods for creating superpatterns of particle deposition were developed (Issle and Hartmann 2008). If the characteristic geometrical dimensions of the areas are comparable to the cell size various interactions occur. In Fig. 8 osteoblasts on garnet layers with different superpatterns of particles are shown. In Fig. 8a stripe patterns of 20 μm width and 20 μm spacing were used. It is clearly visible that the cells align parallel to each other with mutual distances of 20 μm. At higher magnification and after fixation of the cells (removing the aqueous environment by an ethanol series) it becomes obvious that the cells

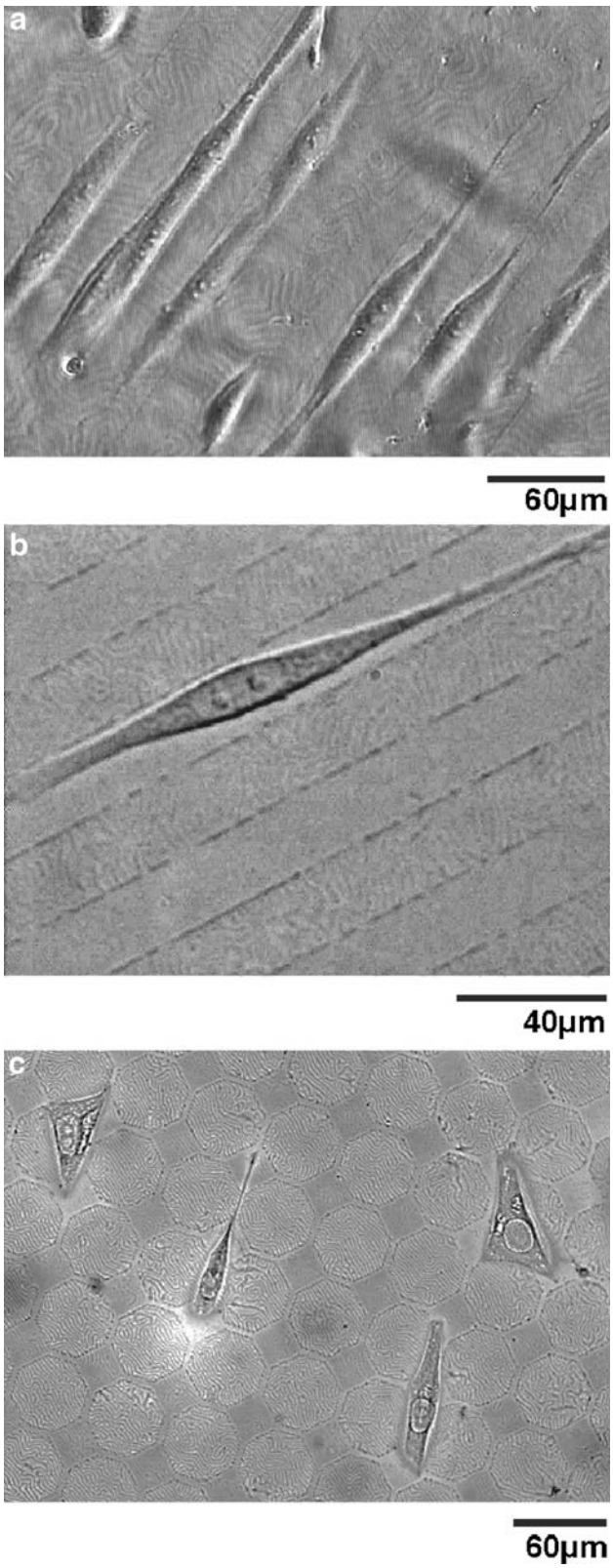

Fig. 8 Anisotropic growth of cells on garnet layers with particles. **a** Osteoblasts on linear areas of particle deposition. They grow in between the 20 µm *broad lines* with deposited beads. **b** The cell avoids contact with the deposited particles. **c** Osteoblasts on an octagon structure. The deposited particles are in the octagons, whereas the cells try to build up focal contacts in areas without beads. This leads to anisotropic growth along an axis or in a triangular shape

grow in between the particle-covered areas (Fig. 8b). The cells seem to avoid contact with the particles completely and they grow in a very elongated spindle-shaped way. The cell width is reduced from approximately 40–50 µm (as seen in Fig. 7) to 15 µm at the core region (Fig. 8), and less than 5 µm at the cell extensions. In order to distinguish between avoiding contact on the one hand and just preferring adhesion to the flat substrate on the other hand a more complex superpattern was chosen. The octagon structures were chosen to induce the growth of one cell per octagon. Therefore, the lattice constant is 50 µm. However, unexpectedly, the cells grow in between the octagons and obviously adhere in the particle-free quadratic areas in the middle of four adjacent octagons (Fig. 8c). Remarkable is the anisotropic growth either along a preferred axis, adhering in successive quadratic areas, or in a triangular shape, utilizing three quadratic areas, respectively. The latter is a proof that cells do not strictly avoid contact with the particles. For the elongated cells the gap between two adjacent octagons is with 2 µm too small and for cells in a triangular pattern the major part of the contact area between cell and substrate is a particle-covered area. In Fig. 8b and c there are black lines at the edges of the structure visible apart from the particles on the domain walls. These lines depend on the particle concentration used during the stamping methods. With rather high particle concentration some of the beads agglomerated at the edges between stamp and substrate. These particular cases were chosen to make the areas of particle deposition visible in light microscopy. Lower particle concentrations led to the same cell behavior at a lower contrast in microscopy.

Cell–surface interaction

In order to explain the anisotropic growth of cells on substrates at particle-free areas and at areas with deposited particles, the physical properties of immobilized particles are relevant. Chemical influences can be neglected since the particles are not functionalized. No chemical modification of the substrate is necessary for particle deposition in geometrically controlled areas compared with uniformly coated garnet layers. Topographical influences in the micron range can also be excluded. The well-known cell behavior of preferred growth on topographical edges (Barbucci et al. 2002) is not observed since the cells do not touch the edges of the structures. They stay in the middle of the lines, or in the case of the octagon structures do not line up along the octagons. Additionally the transition between particle-free areas and areas with particles is not strictly

defined. Due to particle deposition solely on domain walls and not as a compact monolayer there is no compact edge between the naked substrate and particle-covered areas. Accordingly cells should not exhibit any difference in growing on nonstructured substrates, like in Fig. 7, or on superpatterns, like in Fig. 8. The cells grow on the one hand on the particles and avoid it on the other hand if there is the possibility to adhere to the flat substrate. That means cell adhesion is in the present case obviously affected by the nanoscale properties of the particle pattern.

The arrangement of the immobilized particles on the garnet layer exhibits a certain topographic information compared with the atomically flat garnet layer. If a cell adheres to a substrate it must have a tight contact with the material in order to establish connections of integrin ligands to the extracellular matrix (Huang et al. 2004). In the case where the cell must adhere to the particle-covered areas, as in Fig. 7, the situation is more complicated. An integrin complex or a focal adhesion is typically on the order of some μm^2 (Arnold et al. 2004). Thus the cell cannot avoid establishing some adhesion points in direct contact with the particles. The focal adhesions are extended too much to restrict to the center of a domain, where no particles are situated. Assuming a deposition width of 1 μm on top of the domain walls and a domain width of 5 μm, the distance between two adjacent lines of particles is 4 μm, which is of the same order or even smaller than the typical length of a focal adhesion. As a consequence the cell must deform the outer membrane around the particles in order to generate adhesion areas, which is shown schematically in Fig. 9. A calculation of the adhesion energy a cell must spend to change from a spherical shape to an adhesive flat state was performed by Sackmann and Bruinsma (2002). The adhesion state of a cell is characterized in terms of a partially wetting droplet of fluid. Additionally the energy needed in order to bend the membrane, which has a certain elasticity, has to be accounted for. In the present context it is not of primary interest to compare the nonadhering with the adhering cell. It is more relevant to obtain the energy difference ΔE between adhesion on a flat and a rough surface, respectively. Thus, energetic contributions due to membrane deformations at a very small scale and being related to specific adhesion sites do not have to be taken into account. If the membrane thickness is small compared with the respective radius of curvature, the energy ΔE necessary for bending the membrane is given by

$$\Delta E = \frac{1}{2}\kappa \oint \Delta h(x,y)^2 \mathrm{d}A = \frac{1}{2}\kappa \oint \left(\frac{1}{R_1}+\frac{1}{R_2}\right)^2 \mathrm{d}A, \qquad (6)$$

with $R_1$and R_2 characterizing the principal radii of curvature (Sackmann and Bruinsma 2002; Zhong-Can and Helfrich 1989). For simplicity the linear domain structure along the y direction is considered in the following. The cells then do not have to deform along the y direction; thus R_1 is infinite. Deformation yields a radius which is equal to the particles' radius at a total length being equal to the circumference of the particles. This is indicated by the dashed line in Fig. 9. An adhesion site which is related to one particle is thus given by a cylindrical segment of radius R_2 and length $y = 200$ nm. The two-dimensional bending elastic modulus κ of the cell membrane is of the order of 25 k_BT (Sackmann and Bruinsma 2002). Consequently the extra energy resulting from an adhesion to a particle-covered area of the substrate is given by

$$\Delta E = \frac{1}{2}\kappa \oint \left(\frac{1}{R_2}\right)^2 \mathrm{d}A = \frac{\pi y}{2R_2}\kappa \approx 160 k_B T. \qquad (7)$$

Assuming a cell-substrate interface of 800 μm^2 (20 μm width, 40 μm length) this leads to approximately four domain walls, each of a length of 40 μm at a mutual distance of 5 μm, which are covered by one cell. Under these assumptions a cell must additionally spend $\approx 1.28 \times 10^5\ k_BT$ to adhere to particle-covered areas. This might explain why a cell prefers to stay in areas of bare substrate, if available.

Cells on linear stripe domains also show anisotropic growth, as can be seen in Fig. 10. According to the above arguments the cells should grow isotropically because there is no difference from the energetical point of view if they grow along the domain walls or perpendicular to them. The amounts of particles which are covered by the cells are the same in both cases. Thus, there must be an additional energetic reason for anisotropic adherence. Cells build up forces to neighboring cells or to the substrate in order to create tension. This enables stability of the whole tissue under the influence of external forces. The cells tend to grow along directions of maximum stiffness (Lo et al. 2000; Schwarz and Safran 2002; Takakuda and Miyairi

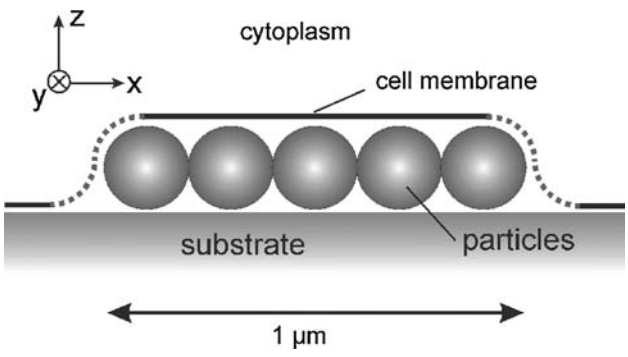

Fig. 9 Schematic drawing explaining the specific cell mechanics. Membrane deformations due to focal contacts on areas with deposited particles are energetically unfavorable for the cell

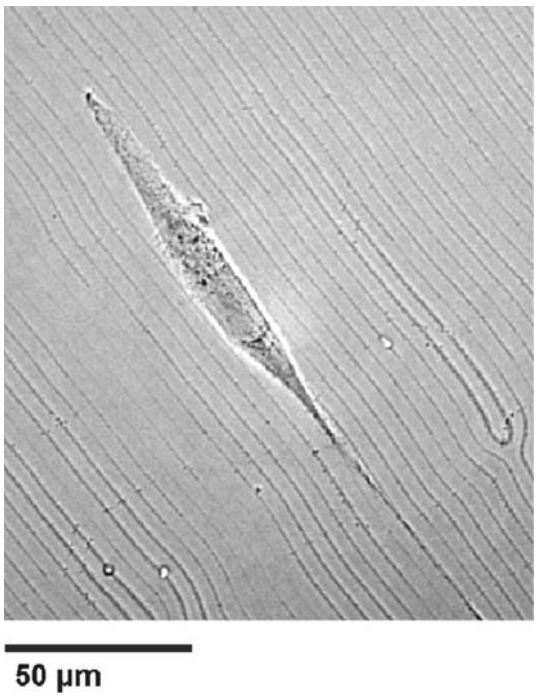

Fig. 10 Osteoblasts show anisotropic growth on particles deposited on stripe domains without further superstructure

1996), which is a consequence of economically establishing tension. The forces exerted via an integrin–fibronectin bond on the surrounding environment are in the range of approximately 5–100 pN (Huang et al. 2004). If a cell establishes a focal complex on top of a particle, the magnetically immobilized particle exhibits a certain elasticity. If there was one single particle on the domain wall it would exhibit a lateral stiffness of $D = 6.7 \times 10^{-4}$ N/m within ±50 nm from the domain wall center. If a cell exerts a force of $F = 10$ pN perpendicular to the domain wall, this leads to a related energy of

$$W = \frac{1}{2D}F^2 \approx 18 k_B T. \quad (8)$$

The particle would be moved by 15 nm perpendicularly to the wall. As the garnet layer exhibits an elastic modulus of about 200 GPa, it can be considered as totally stiff. Thus, apart from an intrinsic energy needed to establish a focal contact, it costs no energy to adhere to the flat substrate, while each contact to a particle requires an energy of about 18 $k_B T$. In the more realistic case where five particles along the cross section of a domain wall are considered, the magnetic adhesion force of the outermost particles is just in the range of 10 pN or even less. It is thus not possible at all for a cell to generate tension by adhering to these elastically bound particles. In the case of complete adhesion of a cell, it can be assumed that on every focal complex the same amount of energy is spent. This leads to anisotropic growth as shown in Fig. 11. The bare substrate or a particle deposition without preferred direction, which is given for the labyrinthine domain structure or the bubbles (Fig. 7), result in the same force on each focal contact. If the cell adheres partly to the bare substrate and partly to particles, the force which can be built up with a given amount of energy is lower on top of the particles because of their elastic binding. As shown schematically in Fig. 11, this can be considered in terms of different springs with different spring constants. This is in agreement with recent observations of cellular behavior on substrates, where the elastic modulus depends on the direction of exerted forces (Bischofs and Schwarz 2003). The anisotropic growth along particles deposited on linear domains, as shown in Fig. 10, can be explained as well: If the domain wall is completely coated, the particles are in mutual contact. This rules out motion of the particles along the walls because of strong frictional forces which occur if many particles are moved simultaneously. The cells thus grow along the walls because no energy is then needed to generate a certain tension.

In general, a newly developed system for cell culturing is introduced. Because of its high variability based on the ability of structural changes in vitro, many future applications arise. The usage of external magnetic fields and magnetic nanoparticles allows for contacting cells via cell–surface interaction in a very controlled manner. Beside the application in clinical diagnostics, e.g., in microfluidic

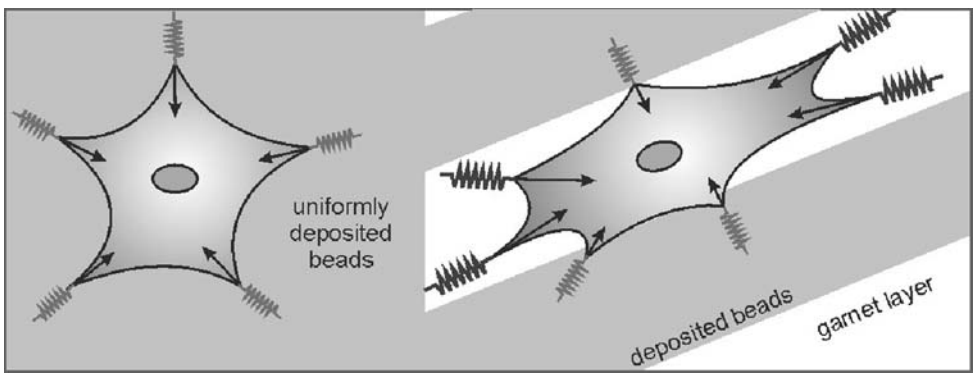

Fig. 11 Schematic drawing of the forces which can be built up by a cell growing on a naked garnet layer or on deposited magnetic particles. The cell can grow isotropically on areas with uniformly deposited beads. Hence superstructures of areas of bead deposition such as lines or octagons lead to anisotropic growth under the assumption of a certain amount of energy required to set up tension in the focal contacts

systems, the system can be used for enabling controlled cell manipulation in fundamental research.

Acknowledgments The authors thank Prof. Tom H. Johansen, Department of Physics, University of Oslo, Norway, for kindly providing the garnet films and AMO, Gesellschaft für Angewandte Mikro- und Optoelektronik mbH in Aachen, Germany, for kindly providing the silicon masters. Also assistance in cell culture and substrate preparation by Susanne Kirsch, Institute of Experimental Physics, Saarland University, is acknowledged. This paper and the work it concerns were generated in the context of the CellPROM project, funded by the European Community as contract No. NMP4-CT-2004-500039 under the 6th Framework Programme for Research and Technological Development.

References

Arnold M, Cavalcanti-Adam EA, Glass R, Blümmel J, Eck W, Kantlehner M, Kessler H, Spatz JP (2004) Activation of integrin function by nanopatterned adhesive interfaces. ChemPhysChem 5:383–388. doi:10.1002/cphc.200301014

Barbucci R, Lamponi S, Magnani A, Pasqui D (2002) Micropatterned surfaces for the control of endothelial cell behaviour. Biomol Eng 19:161–170. doi:10.1016/S1389-0344(02)00022-9

Berry CC, Curtis ASG (2003) Functionalization of magnetic nanoparticles for applications in biomedicine. J Phys D Appl Phys 36:R198–R206. doi:10.1088/0022-3727/36/13/203

Bischofs IB, Schwarz U (2003) Cell organization in soft media due to active mechanosensing. Proc Natl Acad Sci USA 100(16):9274–9279. doi:10.1073/pnas.1233544100

Cavalcanti-Adam EA, Volberg T, Micoulet A, Kessler H, Geiger B, Spatz JP (2007) Cell spreading and focal adhesion dynamics are regulated by spacing of integrin ligands. Biophys J 92:2964–2974. doi:10.1529/biophysj.106.089730

Curtis A, Riehle M (2001) Tissue engineering: the biophysical background. Phys Med Biol 46:R47–R65. doi:10.1088/0031-9155/46/4/201

Curtis A, Wilkinson W (1997) Topographical control of cells. Biomaterials 18(24):1573–1583. doi:10.1016/S0142-9612(97)00144-0

Dalby MJ, Childs S, Riehle MO, Johnstone HJH, Affrossman S, Curtis ASG (2003) Fibroblast reaction to island topography: changes in cytoskeleton and morphology with time. Biomaterials 24:927–935. doi:10.1016/S0142-9612(02)00427-1

Dalby MJ, Riehle MO, Sutherland DS, Agheli H, Curtis ASG (2004) Use of nanotopography to study mechanotransduction in fibroblasts—methods and perspectives. Eur J Cell Biol 83:159–169. doi:10.1078/0171-9335-00369

Huang H, Kamm RD, Lee RT (2004) Cell mechanics and mechanotransduction: pathways, probes and physiology. Am J Physiol Cell Physiol 287:C1–C11. doi:10.1152/ajpcell.00559.2003

Hubert A, Schäfer R (1998) Magnetic domains: the analysis of magnetic microstructures. Springer, Berlin

Hubert A, Malozemoff AP, DeLuca JC (1974) Effect of cubic, tilted uniaxial, and orthorhombic anisotropies on homogenous nucleation in a garnet bubble film. J Appl Phys 45:3562–3571. doi:10.1063/1.1663818

Issle J, Hartmann U (2007) Scanning force microscopy on spatially and temporally varying magnetic substrates for cell cultivation. J Phys Conf Ser 61:487–491. doi:10.1088/1742-6596/61/1/099

Issle J, Hartmann U (2008) Patterning of magnetic nanobeads on surfaces by poly(dimethylsiloxane) stamps. Langmuir 24:888–893. doi:10.1021/la7018956

Issle J, Hartmann U PCT patent application pending. No. WO08014782 A2

Lo CM, Wang HB, Dembo M, Wang YL (2000) Cell movement is guided by the rigidity of the substrate. Biophys J 79:144–152. doi:10.1016/S0006-3495(00)76279-5

Lu AH, Salabas EL, Schüth F (2007) Magnetic nanoparticles: synthesis, protection, functionalization, and application. Angew Chem Int Ed 46:1222–1244. doi:10.1002/anie.200602866

Mrksich M, Whitesides GM (1996) Using self-assembled monolayers to understand the interactions of man-made surfaces with proteins and cells. Annu Rev Biophys Biomol Struct 25:55–78. doi:10.1146/annurev.bb.25.060196.000415

Rejman J, Oberle V, Zuhorn IS, Hoekstra D (2004) Size-dependent internalization of particles via the pathways of clathrin- and caveolae-mediated endocytosis. Biochem J 377:159–169. doi:10.1042/BJ20031253

Sackmann E, Bruinsma RF (2002) Cell adhesion as wetting transition? ChemPhysChem 3:262–269. doi:10.1002/1439-7641(20020315)3:3<262::AID-CPHC262>3.0.CO;2-U

Sato M, Webster TJ (2004) Nanobiotechnology: implications for the future of nanotechnology in orthopedic applications. Expert Rev Med Devices 1(1):105–114. doi:10.1586/17434440.1.1.105

Schwarz AS, Safran SA (2002) Elastic interactions of cells. Phys Rev Lett 88(4):048102 1–4

Takakuda K, Miyairi H (1996) Tensile behaviour of fibroblasts cultured in collagen gel. Biomaterials 17:1393–1397. doi:10.1016/0142-9612(96)87280-2

Teixeira AJ, Abrams GA, Bertics PJ, Murphy CJ, Nealey PP (2003) Epithelial contact guidance on well-defined micro- and nanostructured substrates. J Cell Sci 116(10):1881–1892. doi:10.1242/jcs.00383

Théry M, Racine V, Pépin A, Piel M, Chen Y, Sibarita JB, Bornens M (2006) Anisotropy of cell adhesive microenvironment governs cell internal organization and orientation of polarity. Proc Natl Acad Sci USA 103(52):19771–19776. doi:10.1073/pnas.0609267103

Wong JY, Leach JB, Brown XQ (2004) Balance of chemistry, topography, and mechanics at the cell-biomaterial interface: Issues and challenges for assessing the role of substrate mechanics on cell response. Surf Sci 570:119–133. doi:10.1016/j.susc.2004.06.186

Xia Y, Whitesides GM (1998) Soft lithography. Angew Chem Int Ed 37:550–575. doi:10.1002/(SICI)1521-3773(19980316)37:5<550::AID-ANIE550>3.0.CO;2-G

Yu F, Mücklich F, Li P, Shen H, Mathur S, Lehr CM, Bakowsky U (2005) In vitro cell response to a polymer surface micropatterned by laser interference lithography. Biomacromolecules 6:1160–1167. doi:10.1021/bm049324w

Zhong-Can OY, Helfrich W (1989) Bending energy of vesicle membranes. Phys Rev A 39(10):5280–5288. doi:10.1103/PhysRevA.39.5280